Available online at www.sciencedirect.com
SCIENCE DIRECT®
Earth and Planetary Science Letters 242 (2006) 375–389
EPSL
www.elsevier.com/locate/epsl

Holocene hydrologic balance of tropical South America from oxygen isotopes of lake sediment opal, Venezuelan Andes

P.J. Polissar [a,*], M.B. Abbott [b], A. Shemesh [c], A.P. Wolfe [d], R.S. Bradley [a]

[a] Department of Geosciences, Morrill Science Center, University of Massachusetts, Amherst, MA 01003, USA
[b] Geology and Planetary Science, University of Pittsburgh, Pittsburgh, PA 15260, USA
[c] Environmental Sciences, The Weizmann Institute of Science, Rehovot 76100, Israel
[d] Department of Earth and Atmospheric Sciences, University of Alberta, Edmonton Canada AB T6G 2E3

Received 8 June 2005; received in revised form 21 December 2005; accepted 21 December 2005

Editor: E. Boyle

Abstract

Precipitation in the South American Andes is derived from Atlantic Ocean evaporation which is modified by passage over lowland South America. The isotopic composition of Andean precipitation reflects evaporation conditions over the Atlantic Ocean, moisture recycling during advection across the South American lowlands and uplift to the Andes. Records of the oxygen isotope composition of precipitation in the Venezuelan Andes, derived from lake sediment diatom $\delta^{18}O$ measurements, show a 2.4‰ decrease during the past 10,000 yr. A simple model of the evaporation, advection and uplift processes is used to understand the cause of the isotope shift. The data and model suggest that the decreasing $\delta^{18}O$ reflects a decrease in the fraction of moisture entering South America that reaches the Andes. Ice cores from Peru and Bolivia exhibit similar isotope trends indicating that the shift occurred in both hemispheres. An isotopic record of Amazon River discharge is consistent with the Andean records, indicating increasing continental runoff was associated with the decreasing export of water vapor. Orbital changes in solar insolation cannot explain the synchronous trends in both hemispheres. Changing climate in the tropical Pacific is an attractive explanation for the trends because modern interannual variability in this region has similar effects in both hemispheres.

Keywords: oxygen isotopes; biogenic opal; hydrologic balance; Holocene; Venezuela; Amazon Basin; South America

1. Introduction

The tropical rainforests of South America flourish because of the abundant precipitation they receive. Water balance calculations indicate that approximately 40–50% of the annual precipitation is lost as runoff and the remaining moisture returned to the atmosphere by evaporation and transpiration [1,2]. Transpiration accounts for most of the recycled water vapor [3], intimately linking the hydrologic balance of lowland South America to the vegetation. This interplay between vegetation and climate creates an internal feedback that makes it difficult to predict the impact of external perturbations such as orbital insolation cycles, solar variability and increasing carbon dioxide on the climate of the region. Indeed, the Quaternary evolution

* Corresponding author. Current address: Department of Geosciences, The Pennsylvania State University, 411 Deike Building, University Park, PA 16802, USA. Fax: +1 814 863 7823.
E-mail addresses: polissar@geo.umass.edu, ppolissa@geosc.psu.edu (P.J. Polissar).

0012-821X/$ - see front matter © 2006 Elsevier B.V. All rights reserved.
doi:10.1016/j.epsl.2005.12.024

of the lowlands and their susceptibility to land-use changes and global warming are topics of considerable interest and debate [4–7]. Accordingly, proxy records of past changes in the hydrologic balance of lowland South America are valuable for understanding the ecological and climatic sensitivity of the region.

The isotopic composition of precipitation and atmospheric water vapor is a sensitive indicator of moisture recycling and the atmospheric water balance [8]. Unfortunately there are no long proxy records of the isotopic composition of precipitation in lowland tropical South America. However, atmospheric flow from east-to-west (Fig. 1) transports water vapor from the low elevation tropics to the high Andes where it falls as precipitation, leading to the potential for reconstructing the lowland water balance from proxy records in the Andes. The composition of Andean precipitation integrates the isotopic effects of oceanic evaporation, lowland moisture recycling and orographic uplift. If the impacts of oceanic evaporation and orographic uplift can be constrained, it is then possible to solve for the lowland moisture balance. We explore this potential by reconstructing the isotopic composition of precipitation in the Venezuelan Andes from the oxygen isotope composition of diatom opal preserved in lake sediments. The water balance of northern South America is reconstructed for the past 10,000 yr through modeling the isotopic evolution of water vapor as it is transported from the Atlantic Ocean to the high Andes. The reconstruction is compared to ice core and marine isotope records from tropical South America.

2. Methods and data

2.1. Study site

Laguna Verdes Alta (LVA, 8° 51.17′ N, 70° 52.45′ W, 4215 m) and Baja (LVB, 8° 51.49′ N, 70° 52.42′ W, 4170 m) are small lateral-moraine dammed lakes in the Venezuelan Andes (Fig. 1). Both lakes are groundwater-fed with overland flow contributing water only during heavy precipitation events. LVA has a small outflow stream while LVB has no surface outflow suggesting LVA is hydrologically open while LVB is hydrologically closed. This inference is supported by isotopic analyses of modern surface water samples from the region. On a plot of δD_{lw} vs. $\delta^{18}O_{lw}$, both lakes fall along an evaporative trend below the meteoric water line, however LVB is significantly more enriched than LVA (Fig. 2). The proximity of the lakes means they are subjected to the same climate (humidity, temperature and wind speed) and thermal regime, only differing significantly in their hydrologic balance. There is no evidence for past changes in the strength of the LVA outflow.

Sediment cores were retrieved from the deepest location in LVA (3 m water depth) and LVB (5 m water depth) using a modified square-rod Livingstone corer [9]. Sequential drives were overlapped 10 cm to ensure

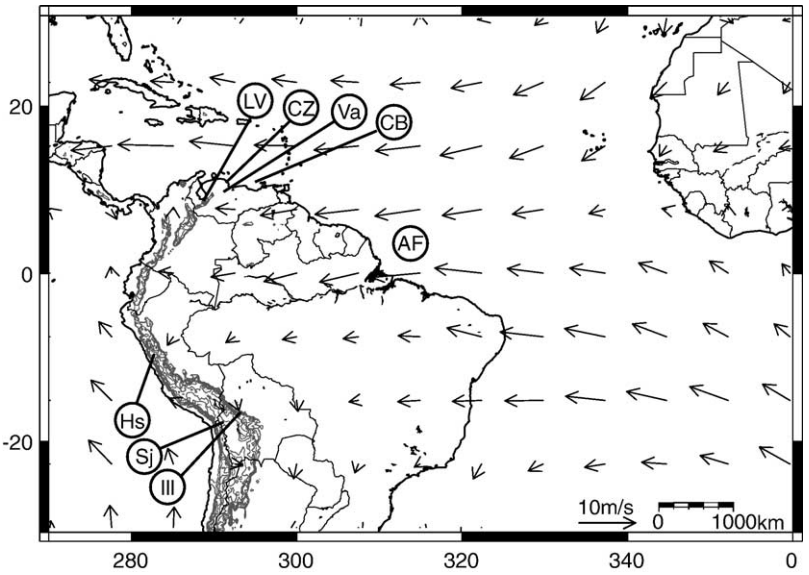

Fig. 1. Location of Laguna Verdes Alta and Baja (LV), Cuevo Zarraga (CZ), Lake Valencia (Va), the Cariaco Basin (CB), Nevados Huascarán (Hs), Sajama (Sj) and Illimani (Ill), and the Amazon Fan (AF). Arrows indicate the direction and magnitude of surface winds (annual average, 1000–850 mb, [28]).

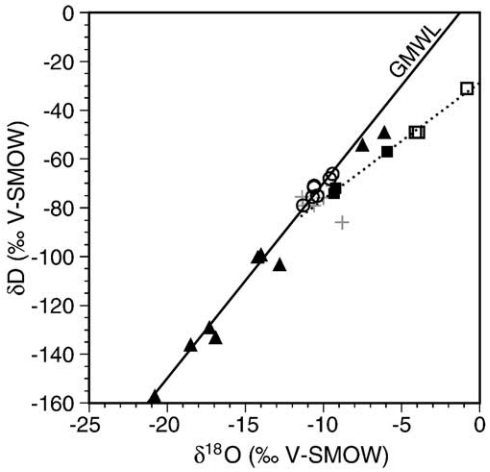

Fig. 2. Oxygen-18 vs. deuterium content of surface waters and precipitation from the Cordillera de Mérida, Venezuela. Precipitation samples (triangles, collected June, 2002), springs (crosses) and hydrologically open lakes (circles) fall along the global meteoric water line (GMWL). Water samples from LVA (filled squares) and LVB (open squares, collected 1999–2002) lie along an evaporative trend below the meteoric water line.

a complete sediment record. Undisturbed sediment/water interface cores were retrieved from both lakes, extruded and sectioned in the field. Variations of total organic carbon (TOC), total nitrogen (TN), $\delta^{13}C_{TOC}$, $\delta^{15}N_{TN}$, atomic C/N ratios and bulk density were used to match sediment depths between the Livingstone and surface cores. Composite sediment records for LVA and LVB were then developed using both the surface and Livingstone cores. The composite core lengths for LVA and LVB are 348 and 373 cm, respectively.

2.2. Sediment chronology

Accelerator mass-spectrometry (AMS) radiocarbon dates from both lakes and an excess ^{210}Pb profile from LVA constrain the age–depth relationship for the cores (Fig. 3; [10]). Radiocarbon ages were converted to calendar ages with the CALIB 4.2 dataset [11,12]. Age models were constructed using the midpoint of the ^{14}C calibration age range with the largest relative area under the probability distribution. Polynomial spline curves were used to interpolate ages between radiocarbon dates. Ages were calculated using the sediment mass accumulation rate and tie points to the LVA record as additional constraints because LVB lacked macrofossil material for ^{14}C dating at most sediment levels. The transition from inorganic glacial material to organic sedimentation occurs at ~15.5 ka BP in both lakes.

2.3. Diatom isotope analyses

Organic matter was removed from sediments with perchloric/nitric acid and diatoms were separated from other oxygen bearing phases by sieving, heavy-liquid density separation and differential settling [13]. Controlled isotope exchange [14] followed by high temperature recrystallization was used to minimize the isotopic effect of opal-bound water. Oxygen was liberated by reaction with BrF_5, released O_2 quantitatively converted to CO_2 and the isotopic composition analyzed via dual-inlet by an upgraded Finnegan MAT 250. The results are calibrated versus NBS-28 quartz international standard and are reported on the VSMOW scale using the standard delta notation:

$$\delta^{18}O_{sample} = \left(\frac{R_{sample}}{R_{VSMOW}} - 1\right) \cdot 10^3 \quad (1)$$

where R is the ratio of ^{18}O/^{16}O. Each sample measurement represents the average of two to four analyses. The median standard deviation of replicate measurements is

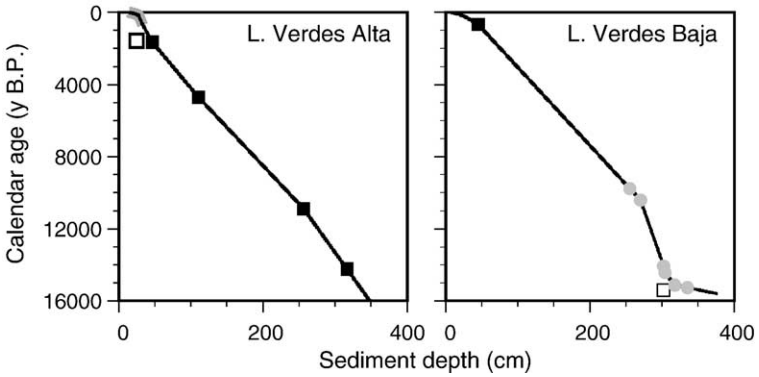

Fig. 3. Age–depth models (thin black line) derived from calibrated AMS radiocarbon ages (solid squares) and ^{210}Pb ages (thick gray line) [10]. Open squares indicate radiocarbon ages not used in age models. The model for LVB is also based upon tie-points (gray circles) with LVA (see Section 2.2).

0.13‰ (n=80) with a range of 0.01–0.53‰. The long term reproducibility is 0.14‰.

2.4. Reconstructing precipitation $\delta^{18}O$ from lake sediments

The isotopic composition of lake water reflects the composition of input water (in this case groundwater) and its modification by evaporative enrichment and atmospheric exchange (governed by the hydrologic balance of the lake). The approach in this paper is to reconstruct the oxygen isotope composition of input water from sediment opal using two lakes with different hydrologic balances to remove the effect of individual lake hydrology. Modern water samples from the study area show that groundwater and non-evaporated surface waters are identical in composition and reflect precipitation without significant modification, therefore, reconstructed input water is used as a proxy for precipitation composition through time.

The steady-state isotopic composition of a lake is described by:

$$\delta_{\text{lake}} = \frac{\delta_a - \delta_{\text{in}} + \varepsilon^* + \left(\frac{1-h}{h}\right) C_k}{1 + \frac{P}{E} k \left(\frac{1-h}{h}\right)} - \delta_{\text{in}} \quad (2)$$

where δ_{lake}, δ_a and δ_{in} are the isotopic composition of lake, atmospheric and inflow waters, h is the relative humidity, ε^* is the equilibrium liquid-vapor fractionation factor [15], C_k the kinetic fractionation factor [16], P/E is the regional precipitation/evaporation ratio and k a constant relating P/E to the input/evaporation ratio (F_{in}/E) of a specific lake ($\frac{F_{\text{in}}}{E} = k\frac{P}{E}$, modified from Gat [16]). Assuming atmospheric water vapor is in isotopic equilibrium with precipitation ($\delta_a = \delta_{\text{in}} - \varepsilon^*$, a reasonable assumption in tropical South America as shown by Matsui et al. [17]), Eq. (2) simplifies to:

$$\delta_{\text{lake}} = \frac{(1-h)(\varepsilon^* + C_k)}{h + (1-h)\frac{P}{E}k} - \delta_{\text{in}} \quad (3)$$

It can be seen from Eq. (3) that diatom $\delta^{18}O$ ($\delta^{18}O_d$) records from two lakes will vary in a 1:1 relationship if they both experience the same input water variations (δ_{in}), regardless of the hydrologic balances of the lakes $\left(\frac{P}{E}k\right)$. Variations of P/E or h will affect hydrologically closed lakes more than open lakes ($k_{\text{closed}} \ll k_{\text{open}}$) and result in unequal $\delta^{18}O_d$ variations. The only other mechanism for a 1:1 variation of $\delta^{18}O_d$ records from two lakes is when the denominator term $(1-h)\frac{P}{E}$ in Eq. (3) remains constant. The evaporation rate from a water surface is approximately proportional to the gradient in relative humidity between the saturated boundary layer directly above the water surface (humidity=1) and the free atmosphere (h) which is $(1-h)$ [18]. Consequently, the evaporation term in $\frac{P}{E}$ is approximately proportional to $(1-h)$, and the term $(1-h)\frac{P}{E}$ can remain constant only if precipitation does not change. Variations in evaporation alone (driven by changes in relative humidity) could potentially cause a 1:1 change in $\delta^{18}O_d$ records from two lakes. However it is likely that a change in evaporation would be accompanied by changes in precipitation and result in unequal shifts in the $\delta^{18}O_d$ of the two records [19].

The diatom opal used to reconstruct lake water $\delta^{18}O$ is subject to a temperature dependent fractionation during formation. Estimates for the magnitude of the temperature fractionation range from −0.2‰/°C to −0.5‰/°C [20–22]. Regardless of the correct value, if two lakes have similar temperature regimes and experience similar temperature variations then changes in $\delta^{18}O_d$ will be identical in both lakes. Located 500 m from each other, LVA and LVB are shallow and unstratified, suggesting they have comparable temperature regimes. Hence, $\delta^{18}O_d$ shifts driven by temperature change should be equal in both lakes. The Holocene trend in the $\delta^{18}O_d$ record from both lakes could be explained by a +5 to +14 °C increase in temperature. However, a pollen record from LVA suggests that temperatures were relatively stable during the Holocene with a possibility for slightly cooler temperatures 8000 to 4500 yr BP [23]. The $\delta^{18}O_d$ could be slightly higher during the Middle Holocene because of this temperature change, however, the Holocene trend is probably not due to temperature change.

The preceding discussion shows that 1:1 variations of the $\delta^{18}O_d$ records from LVA and LVB occur with input water (δ_{in}) and lake water temperature changes. However, lake water temperature changes were likely minimal during the Holocene and the component of the $\delta^{18}O_d$ variations shared by the two lake records is primarily due to changes in the $\delta^{18}O$ of precipitation ($\delta^{18}O_p$) feeding the lakes.

2.5. Modeling $\delta^{18}O$ of precipitation in the Andes

In the tropics, solar heating of the land and ocean leads to a surface low pressure trough, moisture convergence and abundant precipitation. This inter-tropical convergence zone (ITCZ) migrates north and south of the equator following the annual cycle of

solar declination and controls the atmospheric circulation and tropical seasons. Moisture is fed to the ITCZ by nearly zonal (easterly) trade-wind flow close to the trough and more meridional flow at higher latitudes. The easterly trade winds transport air and moisture from the Atlantic Ocean across tropical South America (Fig. 1; see also Fig. 3 in Trenberth [24]). The water vapor content and isotopic composition of this air is modified by precipitation, re-evaporation and runoff during transport across the continent and is further modified during orographic uplift into the Andes (Fig. 4). Predicting the isotopic composition of precipitation in the high Andes involves understanding the processes which occur during evaporation over the Atlantic Ocean, transport across the South American continent and uplift to the high Andes [25,26]. These three steps will be discussed in the following sections.

2.5.1. Oceanic evaporation

At steady state, the isotopic composition of atmospheric water vapor over the ocean is described by:

$$\delta_{atm} = \delta_{ocean} - (\varepsilon^* + (1-h)C_k) \quad (4)$$

where $\varepsilon*$ and C_k are the equilibrium and kinetic isotope effects [18] and h is the boundary layer relative humidity normalized to the ocean water temperature. The key parameters needed to predict δ_{atm} are the ocean water isotopic composition, relative humidity and temperature (which controls ε^*). Values for the oceanic mixed layer $\delta^{18}O$ are available from the NASA/GISS Global Seawater Isotope Database [27]. In the region near tropical South America (30–60° W, 15° S–20° N) the average ocean $\delta^{18}O$ is $+1.00\pm0.15$‰ (average of data in $5°\times5°$ bins). Average oceanic boundary layer temperature and humidity are constrained by data from the NCEP/NCAR reanalysis project [28]. Oceanic sea-surface temperatures from the NODC (Levitus) World Ocean Atlas [29] can be used to normalize boundary layer relative humidity to ocean temperature. Fig. 4 illustrates the effect that large changes in relative humidity have on the $\delta^{18}O$ of marine precipitation.

2.5.2. Lowland recycling

Several authors have described the isotopic evolution of water vapor as it is transported across lowland South America [8,17,30,31]. In its simplest form this process can be described by a Rayleigh equation:

$$\delta_{out} = (\delta_{in} + 1000) f^{(\varepsilon^*-1)} - 1000 \quad (5)$$

where δ_{in} and δ_{out} are the isotopic composition of water vapor entering and leaving the basin, f is the fraction of incoming moisture that leaves the basin (export fraction, $f=F_{out}/F_{in}$) and α^* is the equilibrium vapor–liquid fractionation factor. In a true Rayleigh process all vapor lost from the atmosphere as precipitation would be removed from the system as runoff. However in a real-world model some of the precipitation must be added back to the atmosphere through evapotranspiration from the land surface. The parameter f in Eq. (5) describes the effect of moisture export on the isotopic composition of atmospheric water vapor. The effect of less efficient moisture recycling and export (lower f) is to decrease the ^{18}O content of water vapor leaving the

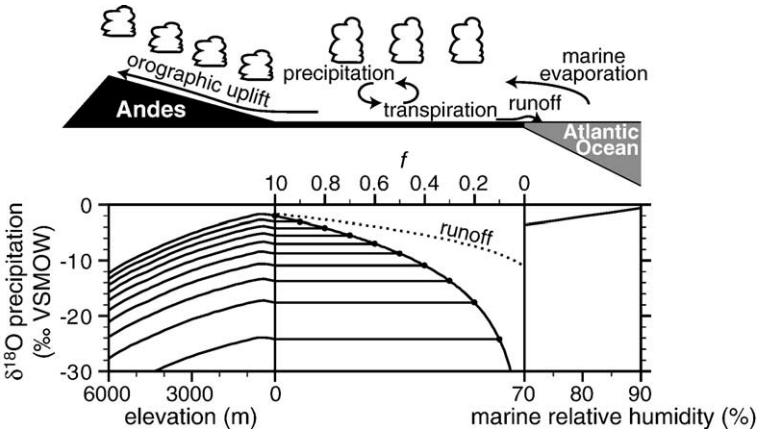

Fig. 4. Schematic of the evaporation, transport and uplift of water vapor from the Atlantic Ocean to the South American Andes (upper panel). The lower panel illustrates variations in the isotopic composition of precipitation expected from changes in the marine boundary layer humidity (right), the fraction of evaporated moisture exported to the Andes (f, center) and the uplift elevation (left). Also shown is the isotopic composition of water lost as runoff.

lowlands (Fig. 4) and increase the amount of incoming moisture (F_{in}) leaving the continent as runoff.

The recycled water is a mixture of transpired and evaporated waters which differ in their isotopic composition: transpiration is non-fractionating ($\delta_T = \delta_p$) while water vapor derived from evaporation is isotopically more negative than the precipitation ($\delta_E < \delta_p$). Because transpired water is isotopically equivalent to the atmospheric moisture from which it is derived, it has no isotopic effect in the Rayleigh formulation above and can be ignored. Isotopic studies indicate that transpiration accounts for 60–80% of the total evapotranspiration in the lowlands [3,32]. In this work we assume that all return flux to the atmosphere is via transpiration (non-fractionating). This assumption simplifies the calculation to a modified Rayleigh equation, but leads to a small systematic underestimate of the export fraction from isotopic data. This bias (discussed below) is small compared to the uncertainty of the evaporation/transpiration ratio in the past and other aspects of the isotope model.

A hidden variable in Eq. (5) is temperature, through its effect on the fractionation factor (α^*). We assume that the fractionation occurs at a temperature of 20 °C, which roughly corresponds to the average lifting condensation level in lowland Venezuela (1200–1500 m). The incoming water vapor (δ_{in}) is assumed to have an isotopic composition equal to the steady-state ocean evaporation $\delta^{18}O$ from Eq. (4).

2.5.3. Orographic uplift and precipitation

Uplift of the air mass to the high Andes is an extension of the Rayleigh distillation process with a variable, temperature dependent fractionation factor. We use the formulation proposed by Pierrehumbert [26] and detailed in Rowley et al. [33], where altitude gradients in temperature and specific humidity are derived from standard meteorological formulae. The isotopic gradient with altitude is then calculated from these values and numerically integrated with height to yield the altitude-isotope relationship. Following Pierrehumbert [26], the liquid–vapor isotopic fractionation factor [15] and saturation vapor pressure relative to water was used for temperatures above 273 K. The ice-vapor fractionation factor and saturation vapor pressure relative to ice were used for temperatures below 253 K. Between 253–273 K, values for the saturation vapor pressure and isotopic fractionation factor were linearly interpolated from the values at 253 and 273 K. This formulation accounts for the coexistence of ice and supercooled water at these temperatures in the deep convective systems typical of tropical precipitation. Kinetic effects during snow formation were ignored but are likely insignificant because most precipitation at the elevation of the lakes in this study falls as rain. Fig. 5 illustrates the vertical gradient of $\delta^{18}O_p$ for different values of the boundary layer water vapor $\delta^{18}O$ (a function of the lowland recycling ratio and oceanic evaporation).

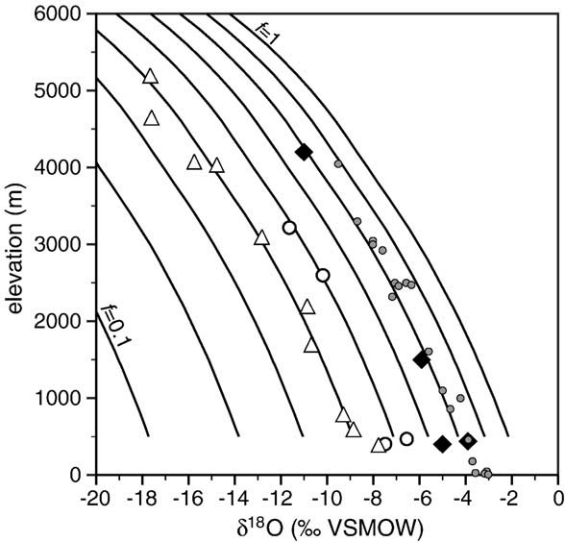

Fig. 5. Altitude–$\delta^{18}O$ gradients for a precipitation integration height 0–1000 m above the ground surface. Each line represents a different lowland recycling ratio (*f*). Precipitation data from two altitude transects of the eastern slope of the Bolivian Andes (open triangles and circles) and Mt. Cameroon (gray circles) are plotted for comparison [35]. The black diamonds are groundwater (400 m a.s.l. near Lake Valencia, [36]), precipitation (Maracay, 442 m and Bocono, 1500 m, [37]) and non-evaporated surface water (4200 m a.s.l., [10]) samples in Venezuela. Gradients were calculated using initial temperature and relative humidity values (24.5 °C, 79%) which provide the best match to surface temperatures in the Venezuela Andes [76].

The boundary conditions which must be known to calculate the altitude–water vapor $\delta^{18}O$ relationship are: the lowland boundary layer temperature, humidity and water vapor $\delta^{18}O$. The boundary layer $\delta^{18}O$ is taken as the output from the Rayleigh fractionation in the lowlands (Eq. (5)). Temperature and humidity are constrained by modern climate data. For past climates we assume that the boundary layer temperature and humidity are determined in the oceanic boundary layer (consistent with the modern data). The effect of variations in temperature and humidity on precipitation $\delta^{18}O$ were investigated in a series of sensitivity experiments detailed below.

Predicting the precipitation $\delta^{18}O$ from the vertical gradient in vapor $\delta^{18}O$ involves and additional variable: precipitation height [26,34]. Precipitation reaching the ground surface does not form at the ground elevation,

rather it originates at some elevation range above that surface. Following Rowley et al. [33], we calculated precipitation weighted averages of $\delta^{18}O_p$ for several elevation ranges above the ground surface (0–1000 to 2000–3000 m at 100 m intervals). We tested these different precipitation height ranges against modern precipitation, surface and groundwater $\delta^{18}O$ data from tropical mountains in Cameroon, Bolivia, Peru [35] and Venezuela [10,36,37]. The optimal fit for the vertical precipitation $\delta^{18}O$ gradient was for precipitation elevations 0–1000 m above the land surface, independent of the absolute $\delta^{18}O_p$ values. When the lowland boundary layer $\delta^{18}O$ is calculated from Eq. (5) using modern climate data, precipitation elevations greater than 0–1000 m give precipitation $\delta^{18}O$ values which are too depleted for the modern precipitation data. We chose therefore to use an integrated precipitation elevation 0–1000 m above the ground surface. The conclusions we draw in this paper are insensitive to the choice of precipitation height if the height has remained constant through time. This is because the isotope shifts we discuss are very similar for all precipitation heights even though the absolute isotope values are different.

3. Discussion

The isotopic records from LVA and LVB have similar Holocene trends towards more negative $\delta^{18}O_d$ values (Fig. 6). The absolute difference in $\delta^{18}O_d$ between LVA and LVB is the result of greater evaporative enrichment of LVB and can be used to infer past variations in the regional moisture balance [10]. Here, we concentrate on the long-term trend shared by both isotope records. This pattern is the result of a change in the isotopic composition of input water (not P/E) and suggests a shift of −2.7‰ in the $\delta^{18}O$ of precipitation during the last 10,000 yr. Changes in the oceanic $\delta^{18}O$, evaporation conditions, the lowland recycling ratio and orographic uplift conditions could all contribute to this shift. The jump from 28.2‰ to 29.3‰ in the isotope values for the upper three data points in LVA appears anomalous given the similarity between the LVA and LVB records prior to these points. It is difficult to hypothesize a climatic process that would cause such a change in LVA and not LVB. We do not have a satisfactory explanation for the shift and do not use these data points in this paper. As a final note, both the short-term shifts and long-term trends in the $\delta^{18}O_d$ records do not correspond to floristic changes in the diatom assemblage. This observation is in accord with previous work showing no inter-species effects on $\delta^{18}O_d$ [21,22].

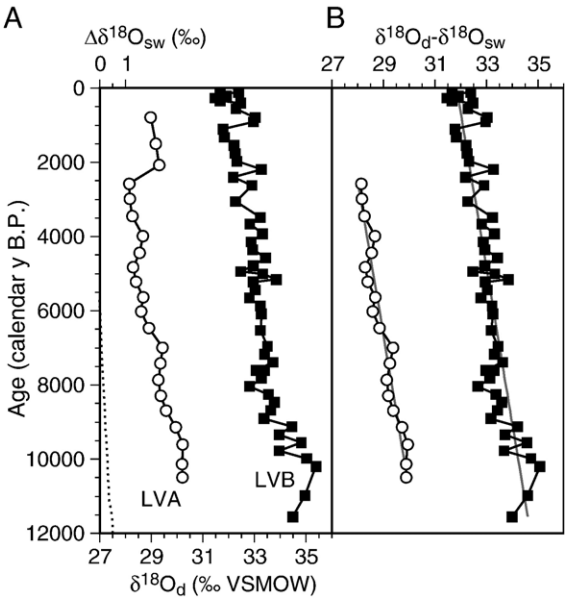

Fig. 6. Diatom $\delta^{18}O$ records from LVA (circles) and LVB (squares) illustrating the trend towards depleted values through the Holocene (A). The dashed line shows how the melting of Pleistocene ice sheets and resulting change in the whole ocean $\delta^{18}O$ would affect the lake isotope records [77,78]. Subtracting the ocean $\delta^{18}O$ change from the $\delta^{18}O_d$ (B) provides an estimate of the Holocene shift in precipitation $\delta^{18}O$ ($2.39*10^{-4}$‰/yr). The upper three data points from LVA are omitted in (B) because they probably do not represent precipitation $\delta^{18}O$ precipitation changes (see Section 3.).

3.1. Ocean evaporation and $\delta^{18}O$

The oceanic $\delta^{18}O$ has decreased by 0.3‰ during the Holocene due to addition of ^{18}O-depleted water from melting Pleistocene ice sheets (Fig. 6). Correcting the diatom $\delta^{18}O$ records for the change in the oceanic reservoir decreases the isotopic shift during the Holocene, however a it leaves a −2.4‰ $\delta^{18}O$ decrease (Fig. 6). Changes in the oceanic surface temperature and/or relative humidity could also affect the $\delta^{18}O$ of moisture advected to South America, and ultimately the $\delta^{18}O_p$ in the Andes. However, an increase in temperature of several tens of degrees would be required to cause a 2.4‰ decrease in the water vapor entering South America (Fig. 7, Table 1), making temperature an unlikely cause of the shift. Corroborating this, sea-surface temperature (SST) records from a number of tropical Atlantic and Caribbean sites show less than 1.5 °C changes during the Holocene [38,39,40]. Alternatively, a decrease of ~16% in the relative humidity of the atmospheric boundary layer would also be sufficient to cause a 2.4‰ decrease in the precipitation $\delta^{18}O$ (Fig. 7). The

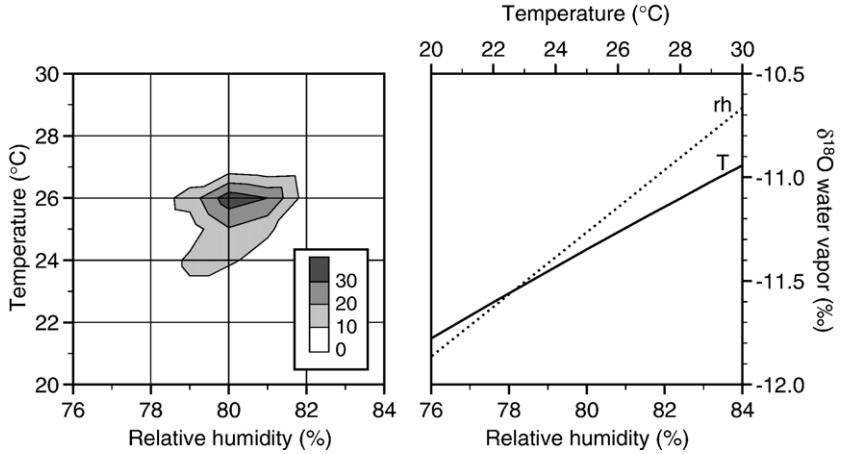

Fig. 7. Frequency distribution of oceanic relative humidity and temperature (left), and the effect of these variables on the $\delta^{18}O$ of marine atmospheric water vapor (right). The frequency distribution ($n=199$) was calculated from annual average Atlantic surface air temperature and relative humidity in the region 20° S–20° N, 285–340° E, excluding land areas [28].

clustering of relative humidity and temperature values in the oceanic source region for S. American water vapor (Fig. 7a) suggests that this is at most a minor cause of isotopic changes over S. America. Given the homogeneity of modern relative humidity and temperature values over the tropical Atlantic even large displacements in atmospheric circulation patterns over the ocean would not have a significant effect.

The inference that changes in oceanic conditions did not cause the isotope shift in the Andes is supported by a speleothem record from coastal Venezuela. The $\delta^{18}O$ of speleothem calcite from Cuevo Zárraga (11° 10.51′ N, 69° 37.68′ W, 960 m; Fig. 2), indicates that the $\delta^{18}O$ of coastal precipitation has been relatively constant during the Holocene (Fig. 10, [41]). This provides empirical support for little or no change in the isotopic composition of water advected into Venezuela during the Holocene (except for the $\delta^{18}O_p$ change due to melting ice-sheets).

3.2. Changing lowland export and precipitation height

Changes in the water balance of the lowlands has a large impact on the isotopic composition of moisture reaching the tropical Andes. We can estimate the modern f ratio (the lowland export fraction) using surface water, ground water and precipitation data from Venezuela (black diamonds in Fig. 5). These data cluster around the altitude–$\delta^{18}O_p$ line for $f=0.8$ suggesting the f ratio in lowland Venezuela is in this range today. Fig. 8 shows the range of precipitation $\delta^{18}O$ values at the elevation of LVA and LVB calculated with different precipitation heights and f ratios. As discussed above, the best fit to modern data puts the precipitation height

Table 1
The sensitivity of Venezuelan Andean precipitation $\delta^{18}O$ at 4200 m to changes in isotope model variables

Variable	Modern value	Sensitivity of $\delta^{18}O_{4200\ m}$ in Andes[a] (‰)	Holocene uncertainty or change	Effect on $\delta^{18}O_{4200\ m}$ (‰)
Ocean $\delta^{18}O$	+1.0‰	+1/‰	−0.3‰	−0.3
Evaporation (T)	26 °C	+0.083/°C	±1 °C	±0.083
Evaporation (rh)	80%	+0.150/%	±2%	±0.3
Lowland export ratio (f)	79%	+0.122/%	−20%	−2.4
Lowland temperature	20 °C	+0.021/°C	±1 °C	±0.021
Lowland evaporation/ evapotranspiration	0%	−0.005 to −0.01/%	±10%	±0.1
Orographic uplift (T)	24.5 °C	+0.359/°C	±1 °C	±0.359
Orographic uplift (rh)	79%	+0.018/%	±2%	±0.036
Precipitation height	0–1000 m	−0.228/100 m	±100 m	±0.228
Wet season/ annual precipitation	80%	−0.040/%	±10%	±0.4

[a] These represent the sensitivity near the modern values. Many equations are nonlinear and the sensitivity changes away from the modern values.

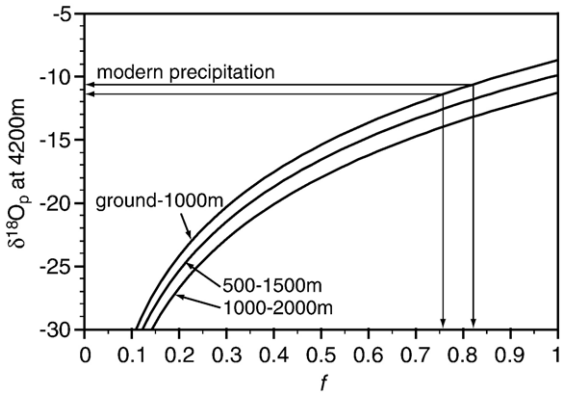

Fig. 8. Oxygen isotopic composition of precipitation at the elevation of LVA and LVB as a function of the elevation above the land surface where the precipitation is derived. The modern precipitation $\delta^{18}O$ indicates a lowland f ratio between 0.76 and 0.82.

at 0–1000 m above the ground surface. Using this range and the modern precipitation $\delta^{18}O$ at LVA–LVB (−10.6‰ to −11.4‰), the modern f ratio is between 0.76 and 0.82. The same calculation for the f ratio 10,000 yr ago yields a range of 0.97 to 1.0. A modern f ratio that is ~78% that of the f ratio 10,000 yr ago is needed to account for a −2.4‰ shift in precipitation at the elevation of LVA–LVB (−2.7‰ corrected for a −0.3‰ change in the oceanic $\delta^{18}O$). This is further illustrated in Fig. 9, which shows the change in the f ratio required to cause a given isotope shift.

Changes in precipitation height have been invoked to explain shifts in the isotopic composition of high-altitude tropical precipitation [34]. It is possible that changes in the precipitation height were responsible for the isotope shift observed in LVA and LVB. An increase in the precipitation height of 945 m would be necessary to cause an isotope change of −2.4‰ during the Holocene. However, the modern precipitation height appears to be just above the surface, requiring the Early Holocene precipitation height to lie below the ground surface. Additionally, it is difficult to justify large changes in precipitation height for the orographically driven upslope precipitation which characterizes the region. Although precipitation height changes cannot be ruled out, the available data suggests they were not the cause of the precipitation $\delta^{18}O$ changes.

3.3. Evapotranspiration and seasonality

In addition to a change in the runoff ratio (f), the decrease of $\delta^{18}O_p$ observed in the Venezuelan Andes could be caused by an increase in the amount of evaporation relative to transpiration in the lowlands. Evaporation returns water to the atmosphere which is depleted in ^{18}O compared to transpired water. Increasing the ratio of evaporation to transpiration would result in a decrease of the $\delta^{18}O_p$ in the Andes. Two lines of evidence suggest this was not an important factor in the decrease. First, a change of evaporation from 0% to 100% of the lowland evapotranspiration can only explain approximately −1.0‰ (calculated using Eq. (7a) in Gat and Matsui [3]) of the −2.4‰ shift in the $\delta^{18}O$ of atmospheric water vapor leaving the lowlands. Clearly this change is unrealistic. Second, vegetation cover (grasslands vs. forest) has a marked impact on the ratio of evaporation to transpiration [42]. However, a lowland pollen record from Lake Valencia, Venezuela (Fig. 1) shows minimal changes in the vegetation cover during the Holocene [43]. Absent vegetation change, it is difficult to explain a large shift in the evaporation/transpiration ratio. These arguments suggest that an increase of the evaporation/transpiration ratio was not a primary cause of the isotopic shift.

The seasonality of precipitation is another factor which may affect the average $\delta^{18}O_p$. At inland tropical locations, precipitation $\delta^{18}O$ during the wet season is more negative than during the dry season. An increase in the contribution of wet-season precipitation to the total precipitation would result in more negative annual averages. Limited data in Venezuela suggests the range of monthly average $\delta^{18}O_p$ is ~8‰ [37] and that the wet season accounts for 80–95% of the annual precipitation near the study site [44]. If the average dry season minus average wet season difference is 8‰,

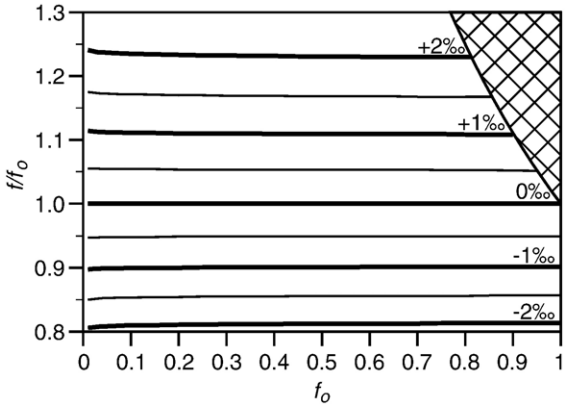

Fig. 9. Changes in the $\delta^{18}O$ of precipitation at the altitude of LVA and LVB expressed as a function if the initial export fraction (f_o) and the fractional change in the export fraction (f/f_o). Although an integration height of 0–1000 m was used for this plot, other integration heights yield nearly identical results. Cross-hatching encompasses f_o–f/f_o pairs which will result in $f>1$.

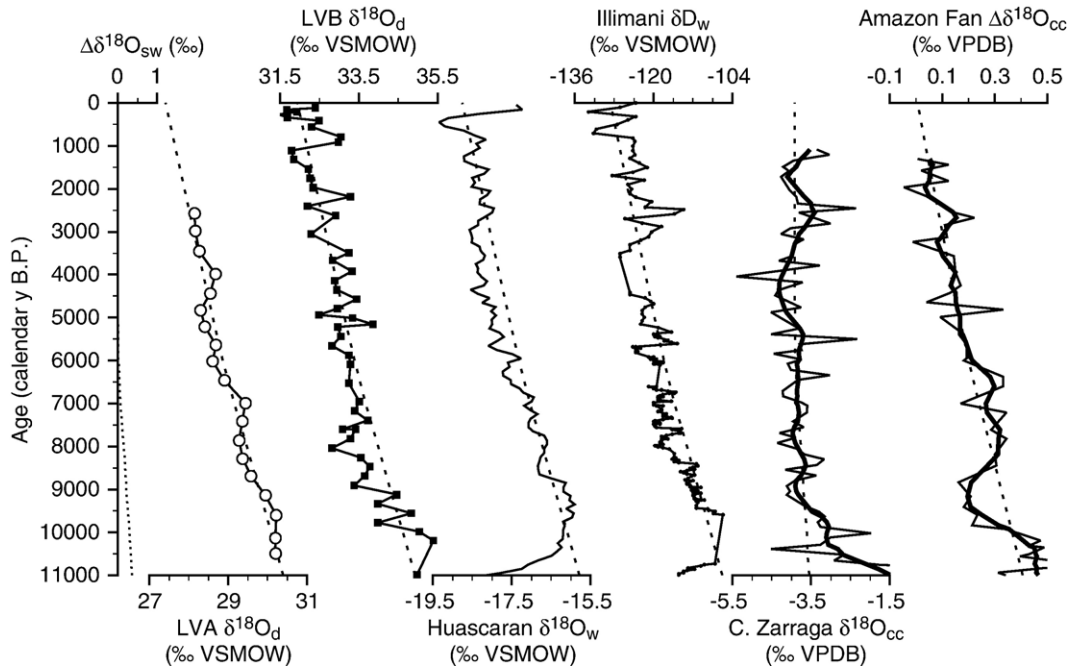

Fig. 10. Isotope records from tropical South America. Materials analyzed include diatom (d) water (w) and calcite (cc) which are reported on either the VSMOW or VPDB international isotope scales. Isotopic shifts are nearly equal on the two scales. The δD record from Illimani was scaled using the ratio of the $\delta^{18}O/\delta D$ equilibrium fractionation factors for vapor–liquid transition (~8). This scaling is validated by measurements of the $\delta^{18}O$ and δD of precipitation and surface waters near Illimani [35,79]. The isotopic shift expected due to changing seawater isotopic composition ($\Delta\delta^{18}O_{sw}$) is shown on the left. Dashed line overlay on each record (except Cuevo Zarraga) indicates an isotopic shift modeled from the LVA and LVB records (see Section 4.). The dashed line over the Cuevo Zarraga record shows the expected $\delta^{18}O_p$ trend from the ocean $\Delta\delta^{18}O_{sw}$ for this coastal location.

isotopic mass-balance calculations indicate that during the Early Holocene the wet-season contribution to the total precipitation would need to be 50–65% to explain the isotope shift. A more realistic scenario, where the difference in the seasonal averages is ~4‰ requires that the Early Holocene wet-season precipitation contribute only 20–35% to the annual total (the smaller wet/dry $\delta^{18}O$ difference better represents the average dry and wet season values compared to the total range of $\delta^{18}O$).

Are such changes in the seasonality of precipitation realistic? In order to produce the isotope shift, dry-season precipitation would have been a dominant source of moisture during the Early Holocene. A longer wet season cannot be invoked because the isotopic composition of this precipitation is more negative, therefore a significant enhancement of dry-season precipitation would have to occur without the ITCZ circulation which provides most precipitation at present. It is difficult to suggest any mechanism which could explain such a shift, and pollen histories from both low-and high-elevation sites in Venezuela do not support a major change in the seasonality of precipitation [23,43].

3.4. Combined effects from several variables

Up to this point only the effects of individual variables on the $\delta^{18}O$ of precipitation in the Andes have been discussed. It is possible that a combination of modest changes in several variables could be responsible for the isotope shift observed in the Venezuelan Andes. Table 1 lists the sensitivity of precipitation $\delta^{18}O$ to all the variables which affect the isotopic composition of Andean precipitation. The $\delta^{18}O$ changes from a combination of all variables sum to ±1.5‰, excluding the ocean $\delta^{18}O$ and the lowland export ratio. Accordingly, reasonable changes in all the variables can only account for ~63% of the isotope shift if they all act in the same manner on the precipitation $\delta^{18}O$. However, there is no a priori reason to suspect that all these variables change in the same manner during the Holocene. Although some variables may have changed together (such as temperature over the ocean, lowlands and during uplift) it is possible that fluctuations in other variables opposed the resulting $\delta^{18}O$ change. Although the uncertainty in the variables affecting precipitation $\delta^{18}O$ increases the uncertainty of

the isotope change explained by the lowland export ratio, the combined uncertainty is considerably less than the total isotope change. Hence, the magnitude of the shift in the lowland export ratio is impacted by the above concerns, but the direction of the change is not in doubt.

4. Reconstructing the continental hydrologic balance

The preceding discussion indicates that a likely cause for the negative shift in $\delta^{18}O_p$ of the Venezuelan Andes lake-isotope records is a decreasing export ratio ($f=F_{out}/F_{in}$) of northern South America. The implication is that the fraction of water vapor entering the continent (F_{in}) which is lost as runoff ($R=F_{in}(1-f)$) has increased during the Holocene. This conclusion indicates changes in the partitioning of moisture between the lowlands and Andes, independent of the absolute intensity of the hydrologic cycle (proportional to F_{in}). In this section we address three questions which arise from this conclusion. First, is the LVA–LVB isotope record a local signal, or does it capture large-scale variations in S. American hydrology? Second, how has the intensity of the hydrologic cycle changed in conjunction with the lowland export ratio? Third, what factor(s) could be responsible for the change in lowland moisture export?

Isotope stratigraphies from three high-altitude ice cores in the tropical Andes are available to compare with the LVA–LVB record (Fig. 1). These isotope records primarily reflect changes in the composition of precipitation, similar to the LVA–LVB data. The data from Huascarán, Peru ([45] with age scale from Thompson [46]) and Illimani, Bolivia [47] bear a striking resemblance to the LVA–LVB record (Fig. 10). Both stratigraphies are dominated by trends that are nearly identical to the LVA–LVB data. In contrast, the isotope record from Sajama, Bolivia (not shown, [48]) shows little trend during the Holocene and is dominated by century-scale variability. Contributions from locally derived water vapor [47] combined with variable wind ablation of surface snow [49] may explain why the Sajama history is so different from the Illimani and Huascarán records. Given the greater proximity of Illimani and Huascarán to the Amazon Basin, we concentrate on the stratigraphies from these sites as more faithful recorders of the isotopic composition of water vapor exported from the lowlands.

The changes of the f ratio during the Holocene inferred from the lake isotope records in the Venezuelan Andes could also explain the isotope shifts observed at Nevados Illimani and Huascarán. To illustrate this we modeled the isotope shifts expected at Illimani and Huascarán if the LVA–LVB record is assumed to be a faithful recorder of changes in the export of lowland moisture to the high Andes. First, the Holocene evolution of the f/f_o ratio was constrained by the $\delta^{18}O_p$–f/f_o relationship in Fig. 9 and a linear fit to the isotope shift in LVA and LVB (Fig. 6). Next, the isotope shift at the elevation of each record was calculated using these f/f_o ratios and the f_o value which provides the best fit to the absolute values of Holocene isotope history (the choice of f_o affects the absolute value, not the shape of the modeled curve). Finally, the $\Delta\delta^{18}O_{sw}$ was added to the modeled isotope values. The results from this modeling exercise fit the ice core isotope records very well (dashed lines, Fig. 10). This fit suggests that the LVA–LVB data is capturing variations in the lowland hydrology which occurred throughout tropical S. America.

As an additional exercise, the isotopic composition of Amazon River water was calculated using the f/f_o history inferred from the LVA–LVB record and compared to an isotope record of Amazon River discharge during the Holocene. The calculation used a value for f_o (0.45) which provides the correct isotope signature for the modern Amazon River (−5‰ VSMOW, [50]). This calculated runoff record was then corrected for the $\Delta\delta^{18}O_{sw}$ and the amount of runoff was assumed proportional to $(1-f)$ (from mass balance). Finally, the isotopic composition of a mixture of Amazon River and ocean water ($\Delta\delta^{18}O$) was calculated for comparison to a $\Delta\delta^{18}O$ record from the Amazon Fan [50]. This mixing calculation was scaled to the modern ratio of ocean to river water at the coring site (5 : 1) by using the equation:

$$\Delta\delta_{mix} = \left(5\delta_{ocean} + \frac{1-f(t)}{1-f_o}\delta_{river}\right) \Big/ \left(5 + \frac{1-f(t)}{1-f_o}\right) \quad (6)$$

where $f(t)$ is the f ratio at time t (derived from the LVA–LVB record). Comparison of the modeled and measured isotope shifts shows a strong correspondence (Fig. 10). This exercise suggests that the increase in Amazon River discharge inferred from the Amazon Fan record [50] could be the result of a shift in the partitioning of moisture between the Andes and the Amazon Basin. Additionally, the $\Delta\delta^{18}O$ shift observed in the Amazon Fan record is consistent with the Andean records of $\delta^{18}O_p$, without invoking any change in the intensity of the hydrologic cycle.

Similarities between the Holocene $\delta^{18}O_p$ records from both hemispheres of tropical S. America intimate that there might be a single underlying cause.

Possibilities include changes in the oceanic source regions, continental temperature changes, vegetation changes in the lowlands (moisture recycling) and circulation shifts driven directly by orbital variations of solar insolation or indirectly through teleconnections with other regions. As discussed previously for the LVA–LVB record, there is no evidence for Holocene changes in the oceanic source regions which could explain the isotope shifts observed in the Andes. Additionally, although continental temperatures could affect the isotope records by altering the vapor/liquid fractionation during precipitation, the required temperature changes are quite large and no paleoclimate evidence supports such changes. A shift from forest to savanna in the tropical lowlands during the Holocene would decrease transpiration and increase evaporation and runoff, possibly decreasing the export ratio (f) and the $\delta^{18}O_p$ in the Andes. However, pollen records from lowland tropical S. America do not support the large change in vegetation coverage which would be required to cause the isotope shifts [43,51,52]. Finally, orbitally caused insolation changes could be invoked to directly explain either the northern or southern hemisphere isotope records. However the effect of precessional insolation forcing is opposite in the northern and southern hemispheres suggesting that direct insolation forcing of climate changes is not a likely source of the similar isotope trends in the Andes of both hemispheres.

Shifts in tropical S. America atmospheric circulation driven by changes in the equatorial Pacific SST may provide a unifying explanation for the isotope trends observed in the Andean records. Interannual variations of SSTs in the eastern equatorial Pacific have an important effect on the moisture transport and the amount and isotopic composition of precipitation in tropical S. America (based upon instrumental records). Warmer SSTs and stronger latitudinal temperature gradients in the eastern equatorial Pacific cause westerly anomalies in upper tropospheric winds over S. America leading to decreased precipitation during the austral summer in the southern hemisphere Andes [53–55]. Precipitation in the lowlands also decreases [53,56] leading to less rainout, higher f ratios and a higher $\delta^{18}O$ of precipitation in the Andes [35,57–60]. In Venezuela and northern S. America, higher SSTs in the eastern equatorial Pacific also lead to reduced precipitation during the boreal summer [53,61,62]. Climate model experiments suggest the relationship between eastern equatorial Pacific SST variability and $\delta^{18}O_p$ in northern S. America is similar to the southern hemisphere tropics [63] making eastern equatorial Pacific variability an attractive explanation for the synchronous changes in both hemispheres.

Applying the relationship between modern interannual variability of Pacific SSTs and the $\delta^{18}O$ of Andean precipitation to the observed changes in the Holocene isotope stratigraphies from the tropical Andes suggests that higher isotope values during the Early Holocene resulted from warmer temperatures in the eastern equatorial Pacific. However, this does not agree with paleoclimate data and global climate model (GCM) experiments which suggests that the eastern equatorial Pacific was generally cooler during the Early Holocene [64–67]. However, the relationship of interannual variability and the mean conditions of eastern equatorial Pacific SSTs to the S. American water cycle on millennial time scales is probably not straightforward. The interannual variability which dominates SSTs in the eastern equatorial Pacific today may not be a good model for millennial-scale shifts in the mean state of the tropical Pacific. Additionally, asymmetric response of the continental water cycle to warm and cold events (c.f. [68]) could cause a directional response to increased variability, even if the mean remains unchanged. Although paleoclimate data and climate models suggest that interannual SST variability in the eastern equatorial Pacific was lower during the Early Holocene (e.g., [69–73]), there is some evidence to the contrary [67]. It should also be noted that some records from the eastern equatorial Pacific do indicate warmer conditions during the Early Holocene [74,75], consistent with the Andean isotope histories.

While acknowledging the complexities which link SST variations in the equatorial Pacific to the hydrologic cycle of tropical S. America, we suggest that it is difficult to explain the similarity of precipitation isotope records north and south of the equator by another mechanism. Better understanding of how changes in the Pacific Ocean affect S. American climate on millennial time scales may strengthen or weaken this interpretation of the Andean isotope records. Additional records of the isotopic composition of precipitation in S. America during the Holocene may also shed light by revealing regional differences which are not apparent in the available data.

5. Summary and conclusions

Diatom isotope records from two lakes in the Venezuelan Andes indicate a −2.4‰ shift in the $\delta^{18}O$ of Andean precipitation during the Holocene. This shift could be caused by changes in ocean evaporation conditions, transport across lowland S. America or orographic uplift to the Andes. However, several lines of evidence suggest that a change in the efficiency of water vapor transport across the lowlands is responsible for

the shift. Ice cores from Nevados Huascarán, Peru and Illimani, Bolivia exhibit isotope trends which are very similar to the Venezuelan record suggesting the changes occurred in both hemispheres of tropical S. America. The interhemispheric similarity of the isotope records makes orbitally driven trends in solar insolation an unlikely primary cause for the shifts. Modern interannual variability in the equatorial Pacific Ocean has similar climate effects in both hemispheres of tropical S. America making variability in this region an attractive explanation for the isotope trends. However, the interpretation of the millennial scale isotope histories based upon the modern teleconnections between the tropical Pacific and S. America does not agree with available paleoclimate evidence from the tropical Pacific. This may reflect additional complexity in the relationship between tropical Pacific interannual and millennial scale variability and its effects on the hydrologic cycle of S. America. We favor a tropical Pacific source for the isotope trends but better understanding of the teleconnection between the Pacific and S. America are needed to test this theory.

Acknowledgments

Funding for this research provided by the U.S.-N.S.F. (ATM 98-08943, ATM 98-08943, OISE-0004425), Geological Society of America and Department of Geosciences, University of Massachusetts. We thank Ruth Yam and Irena Brailovsky at the Weizmann Institute of Science for diatom isotopic analyses. Dr. Maximiliano Bezada was instrumental in the sample collection for this study. The suggestions of an anonymous review helped strengthen the manuscript.

References

[1] E. Salati, The climatology and hydrology of Amazonia, in: G.T. Prance, T.E. Lovejoy (Eds.), Amazonia, Pergamon Press, New York, 1985, pp. 18–48.
[2] M.H. Costa, J.A. Foley, Trends in the hydrologic cycle of the Amazon Basin, J. Geophys. Res.-Atmos. 104 (1999) 14189–14198.
[3] J.H. Gat, E. Matsui, Atmospheric water balance in the Amazon Basin: an isotopic evapotranspiration model, J. Geophys. Res. 96 (1991) 13,179–113,188.
[4] P.A. Colinvaux, G. Irion, M.E. Räsänen, M.B. Bush, J.A.S. Nunes de Mello, A paradigm to be discarded: geological and paleoecological data falsify the HAFFER & PRANCE refuge hypothesis of Amazonian speciation, Amazoniana XVI (2001) 609–646.
[5] M.B. Bush, M.C. Miller, P.E. De Oliveira, P.A. Colinvaux, Orbital forcing signal in sediments of two Amazonian lakes, J. Paleolimnol. 27 (2002) 341–352.
[6] A. Henderson-Sellers, K. McGuffie, H. Zhang, Stable isotopes as validation tools for global climate model predictions of the impact of Amazonian deforestation, J. Climate 15 (2002) 2664–2677.
[7] S. Curtis, S. Hastenrath, Trends of upper-air circulation and water vapour over equatorial South America and adjacent oceans, Int. J. Climatol. 19 (1999) 863–876.
[8] J.R. Gat, Atmospheric water balance—the isotopic perspective, Hydrol. Process. 14 (2000) 1357–1369.
[9] H.E. Wright, D.H. Mann, P.H. Glaser, Piston corers for peat and lake sediments, Ecology 65 (1984) 657–659.
[10] P.J. Polissar, Lake records of Holocene climate change, Cordillera de Mérida, Venezuela, Ph.D., University of Massachusetts, 2005.
[11] M. Stuiver, P.J. Reimer, T.F. Braziunas, High-precision radiocarbon age calibration for terrestrial and marine samples, Radiocarbon 40 (1998) 1127–1151.
[12] M. Stuiver, P.J. Reimer, E. Bard, J.W. Beck, G.S. Burr, K.A. Hughen, B. Kromer, F.G. McCormac, J.v.d. Plicht, M. Spurk, INTCAL98 radiocarbon age calibration 24,000–0 cal BP, Radiocarbon 40 (1998) 1041–1083.
[13] A. Shemesh, L.H. Burckle, J.D. Hays, Late Pleistocene oxygen isotope records of biogenic silica from the Atlantic sector of the Southern Ocean, Paleoceanography 10 (1995) 179–196.
[14] A. Juillet-Leclerc, L. Labeyrie, Temperature dependence of the oxygen isotopic fractionation between diatom silica and water, Earth Planet. Sci. Lett. 84 (1987) 69–74.
[15] J. Horita, D.J. Wesolowski, Liquid–vapor fractionation of oxygen and hydrogen isotopes of water from the freezing to the critical temperature, Geochim. Cosmochim. Acta 58 (1994) 3425–3437.
[16] J.R. Gat, Stable isotopes of fresh and saline lakes, in: A. Lerman, D.M. Imboden, J.R. Gat (Eds.), The Physics and Chemistry of Lakes, Springer-Verlag, New York, 1995, pp. 139–164.
[17] E. Matsui, E. Salati, M.N.G. Ribeiro, C.M. Reis, A.C.S.N.F. Tancredi, J.R. Gat, Precipitation in the central Amazon Basin—the isotopic composition of rain and atmospheric moisture at Belém and Manaus, Acta Amazon. 13 (1983) 307–369.
[18] H. Craig, L.I. Gordon, Deuterium and oxygen-18 variations in the ocean and the marine atmosphere, in: E. Tongiorgi (Ed.), Stable Isotopes in Oceanographic Studies and Paleotemperatures, Consiglio Nazionale delle Richerche, Laboratorio di Geologica, Pisa, 1965.
[19] A. Shemesh, D. Peteet, Oxygen isotopes in fresh water biogenic opal—Northeastern US Alleröd–Younger Dryas temperature shift, Geophys. Res. Lett. 25 (1998) 1935–1938.
[20] A. Shemesh, C.D. Charles, R.G. Fairbanks, Oxygen isotopes in biogenic silica: global changes in ocean temperature and isotopic composition, Science 256 (1992) 1434–1436.
[21] M.E. Brandriss, J.R. O'Neil, M.B. Edlund, E.F. Stoermer, Oxygen isotope fractionation between diatomaceous silica and water, Geochim. Cosmochim. Acta 62 (1998) 1119–1125.
[22] R. Moschen, A. Lücke, G.H. Schleser, Sensitivity of biogenic silica oxygen isotopes to changes in surface water temperature and paleoclimatology, Geophys. Res. Lett. 32 (2005), doi:10.1029/2004GL022167.
[23] V. Rull, M.B. Abbott, P.J. Polissar, A.P. Wolfe, M. Bezada, R.S. Bradley, High altitude vegetation change during the last 15,000 years in the tropical Andes: the pollen record of Laguna Verde Alta, Venezuela, Quat. Res. 64 (2005) 308–317.

[24] K.E. Trenberth, Atmospheric moisture recycling: role of advection and local evaporation, J. Climate 12 (1999) 1368–1381.
[25] P.M. Grootes, M. Stuiver, Oxygen isotope changes in tropical ice, Quelccaya, Peru, J. Geophys. Res. 94 (1989) 1187–1194.
[26] R.T. Pierrehumbert, Huascaran $\delta^{18}O$ as an indicator of tropical climate during the Last Glacial Maximum, Geophys. Res. Lett. 26 (1999) 1345–1348.
[27] G.A. Schmidt, G.R. Bigg, E.J. Rohling, Global seawater oxygen-18 database, NASA/GISS, http://www.giss.nasa.gov/data/o18data/, 1999.
[28] E. Kalnay, M. Kanamitsu, R. Kistler, W. Collins, D. Deaven, L. Gandin, M. Iredell, S. Saha, G. White, J. Woollen, Y. Zhu, M. Chelliah, W. Ebisuzaki, W. Higgins, J. Janawiak, K.C. Mo, C. Ropelewski, J. Wang, A. Leetmaa, R. Reynolds, R. Jenne, D. Joseph, The NCEP/NCAR reanalysis 40-year project, Bull. Am. Meteorol. Soc. 77 (1996) 437–471.
[29] NODC, NODC (Levitus) World Ocean Atlas, NOAA–CIRES Climate Diagnostic Center, Boulder, Colorado, USA, 1998.
[30] E. Salati, A. Dall'Olio, E. Matsui, J.R. Gat, Recycling of water in the Amazon Basin: an isotopic study, Water Resour. Res. 15 (1979) 1250–1258.
[31] L.A. Martinelli, R.L. Victoria, L.S.L. Sternberg, A. Ribeiro, M.Z. Moreira, Using stable isotopes to determine sources of evaporated water to the atmosphere in the Amazon Basin, J. Hydrol. 183 (1996) 191–204.
[32] R.L. Victoria, L.A. Martinelli, J. Mortatti, J. Richey, Mechanisms of water recycling in the Amazon Basin: isotopic insights, Ambio 20 (1991) 384–387.
[33] D.B. Rowley, R.T. Pierrehumbert, B.S. Currie, A new approach to stable isotope-based paleoaltimetry: implications for paleoaltimetry and paleohypsometry of the High Himalaya since the Late Miocene, Earth Planet. Sci. Lett. 188 (2001) 253–268.
[34] L.G. Thompson, E. Mosley-Thompson, K.A. Henderson, Ice-core palaeoclimate records in tropical South America since the Last Glacial Maximum, J. Quat. Sci. 15 (2000) 377–394.
[35] R. Gonfiantini, M.-A. Roche, J.-C. Olivry, J.-C. Fontes, G.M. Zuppi, The altitude effect on the isotopic composition of tropical rains, Chem. Geol. 181 (2001) 147–167.
[36] K.-P. Seiler (Ed.), Man's Impact on the Groundwater Systems, IAEA, Vienna, Germany, 2000, 106 pp.
[37] IAEA/WMO, Global network of isotopes in precipitation. The GNIP database, Accessible at: http://isohis.iaea.org, 2001.
[38] C. Rühlemann, S. Mulitza, P.J. Müller, G. Wefer, R. Zahn, Warming of the tropical Atlantic Ocean and slowdown of the thermohaline circulation during the last deglaciation, Nature 402 (1999) 511–514.
[39] D.W. Lea, D.K. Pak, L.C. Peterson, K.A. Hughen, Synchroneity of tropical and high-latitude Atlantic temperatures over the last glacial termination, Science 301 (2003) 1361–1364.
[40] M. Schmidt, H.J. Spero, D.W. Lea, Links between salinity variation in the Caribbean and North Atlantic thermohaline circulation, Nature 428 (2004) 160–163.
[41] L.A. González, R. Gómez, High resolution speleothem paleoclimatology of northern Venezuela: a progress report, Bol. Soc. Venez. Espeleol. 36 (2002) 27–29.
[42] M.Z. Moreira, L.S.L. Sternberg, L.A. Martinelli, R.L. Victoria, E.M. Barbosa, L.C. Bonates, D.C. Nepstad, Contribution of transpiration to forest ambient vapour based upon isotopic measurements, Glob. Chang. Biol. 3 (1997) 439–450.
[43] J.P. Bradbury, B. Leyden, M. Salgado-Labouriau, W.M. Lewis Jr., C. Schubert, M.W. Binford, D.G. Frey, D.R. Whitehead, F.H. Weibezahn, Late Quaternary environmental history of Lake Valencia, Venezuela, Science 214 (1981) 1299–1305.
[44] A. Azocar, M. Monasterio, Caracterización ecológica del clima en El Páramo de Mucubají, in: M. Monasterio (Ed.), Estudios Ecologicos en los Páramos Andinos, Ediciones de la Universidad de Los Andes, Merida, Venezuela, 1980, pp. 207–223.
[45] L.G. Thompson, E. Mosley-Thompson, M.E. Davis, P.-N. Lin, K.A. Henderson, J. Cole-Dai, J.F. Bolzan, K.-b. Liu, Late Glacial Stage and Holocene tropical ice core records from Huascarán, Peru, Science 269 (1995) 46–50.
[46] L.G. Thompson, Huascaran ice core data, IGBP PAGES/World Data Center A for Paleoclimatology, Data Contribution Series #2001-008, NOAA/NGDC Paleoclimatology Program, Boulder CO, USA, 2001.
[47] E. Ramirez, G. Hoffman, J.D. Taupin, B. Francou, P. Ribstein, N. Caillon, F.A. Ferron, A. Landais, J.R. Petit, Pouyaud, U. Schotterer, J.C. Simmoes, M. Stievenard, A new Andean deep ice core from Nevado Illimani (6350 m), Bolivia, Earth Planet. Sci. Lett. 212 (2003) 337.
[48] L.G. Thompson, M.E. Davis, E. Mosley-Thompson, T.A. Sowers, K.A. Henderson, V.S. Zagorodnov, P.-N. Lin, V.N. Mikhalenko, R.K. Campen, J.F. Bolzan, J. Cole-Dai, B. Francou, A 25,000-year tropical climate history from Bolivian ice cores, Science 282 (1998) 1858–1864.
[49] D.R. Hardy, M. Vuille, R.S. Bradley, Variability of snow accumulation and isotopic composition on Nevado Sajama, Bolivia, J. Geophys. Res. 108 (2003), doi:10.1029/2003JD003623.
[50] M.A. Maslin, S.J. Burns, Reconstruction of the Amazon Basin effective moisture availability over the past 14,000 years, Science 290 (2000) 2285–2287.
[51] S.G. Haberle, M.A. Maslin, Late Quaternary vegetation and climate change in the Amazon Basin based on a 50,000 year pollen record from the Amazon Fan, ODP Site 932, Quat. Res. 51 (1999) 27–38.
[52] F.E. Mayle, D.J. Beerling, Late Quaternary changes in Amazonian ecosystems and their implications for global carbon cycling, Palaeogeogr. Palaeoclimatol. Palaeoecol. 214 (2004) 11–25.
[53] P. Aceituno, On the functioning of the Southern Oscillation in the South American sector. Part I. Surface climate, Mon. Weather Rev. 116 (1988) 505–524.
[54] M. Vuille, Atmospheric circulation over the Bolivian Altiplano during dry and wet periods and extreme phases of the Southern Oscillation, Int. J. Climatol. 19 (1999) 1579–1600.
[55] R.D. Garreaud, M. Vuille, A.C. Clement, The climate of the Altiplano: observed current conditions and mechanisms of past changes, Palaeogeogr. Palaeoclimatol. Palaeoecol. 194 (2003) 5–22.
[56] B. Lyon, The strength of El Niño and the spatial extent of tropical drought, Geophys. Res. Lett. 31 (2004), doi:10.1029/2004GL020901.
[57] M. Vuille, R.S. Bradley, R. Healy, M. Werner, D. Hardy, L.G. Thompson, F. Keimig, Modeling the $\delta^{18}O$ in precipitation over the tropical Americas. 2. Simulation of the stable isotope signal in Andean ice cores, J. Geophys. Res. 108 (2003), doi:10.1029/2001JD002039.
[58] R.S. Bradley, M. Vuille, D. Hardy, L.G. Thompson, Low latitude ice cores record Pacific sea surface temperatures, Geophys. Res. Lett. 30 (2003), doi:10.1029/2002GL016546.
[59] G. Hoffmann, E. Ramirez, J.D. Taupin, B. Francou, P. Ribstein, R. Delmas, H. Drr, R. Gallaire, J. Simes, U. Schotterer, M. Stievenard, M. Werner, Coherent isotope history of Andean ice

cores over the last century, Geophys. Res. Lett. 30 (2003), doi:10.1029/2002GL014870.
[60] S. Hastenrath, D. Polzin, B. Francou, Circulation variability reflected in ice core and lake records of the southern tropical Andes, Clim. Change 64 (2004) 361–375.
[61] R.S. Pulwarty, R.G. Barry, H. Riehl, Annual and seasonal patterns of rainfall variability over Venezeula, Erdkunde 46 (1992) 273–289.
[62] D.B. Enfield, Relationship of inter-American rainfall to tropical Atlantic and Pacific SST variability, Geophys. Res. Lett. 23 (1996) 3305–3308.
[63] M. Vuille, R.S. Bradley, M. Werner, R. Healy, F. Keimig, Modeling $\delta^{18}O$ in precipitation over the tropical Americas. 1. Interannual variability and climatic controls, J. Geophys. Res. 108 (2001), doi:10.1029/2001JD002038.
[64] A.B.G. Bush, Assessing the impact of Mid-Holocene insolation on the atmosphere–ocean system, Geophys. Res. Lett. 26 (1999) 99–102.
[65] A. Kitoh, S. Murakami, Tropical Pacific climate at the Mid-Holocene and the Last Glacial Maximum simulated by a coupled ocean–atmosphere general circulation model, Paleoceanography 17 (2002), doi:10.1029/2001PA000724.
[66] Z. Liu, E. Brady, J. Lynch-Stieglitz, Global ocean response to orbital forcing in the Holocene, Paleoceanography 18 (2003) 1041–1081.
[67] M. Carré, I. Bentaleb, M. Fontugne, D. Lavallée, Strong El Niño events during the Early Holocene: stable isotope evidence from Peruvian sea shells, Holocene 15 (2005) 42–47.
[68] G. Poveda, O.J. Mesa, Feedbacks between hydrological processes in tropical South America and large-scale ocean–atmospheric phenomena, J. Climate 10 (1997) 2690–2702.
[69] A.C. Clement, R. Seager, M.A. Cane, Suppression of El Niño during the Mid-Holocene by changes in the Earth's orbit, Paleoceanography 15 (2000) 731–737.
[70] D.H. Sandweiss, K.A. Maasch, R.L. Burger, J.B. Richardson III, H.B. Rollins, A. Clement, Variation in Holocene El Niño frequencies: climate records and cultural consequences in ancient Peru, Geology 29 (2001) 603–606.
[71] A.W. Tudhope, C.P. Chilcott, M.T. McCulloch, E.R. Cook, J. Chappel, R.M. Ellam, D.W. Lea, J.M. Lough, G.B. Shimmield, Variability in the El Niño–Southern Oscillation through a glacial–interglacial cycle, Science 291 (2001) 1511–1517.
[72] C.M. Moy, G. Seltzer, D.T. Rodbell, D. Anderson, Variability of El Niño/Southern Oscillation activity at millennial time scales during the Holocene epoch, Nature 420 (2002) 162–165.
[73] A. Koutavas, J. Lynch-Stieglitz, Glacial–interglacial dynamics of the eastern equatorial Pacific cold tongue–intertropical convergence zone system reconstructed from oxygen isotope records, Paleoceanography 18 (2003), doi:10.1029/2003PA000894.
[74] D.W. Lea, D.K. Pak, H.J. Spero, Climate impact of Late Quaternary equatorial Pacific sea surface temperature variations, Science 289 (2000) 1719–1724.
[75] P. Loubere, M. Richaud, Z. Liu, F. Mekik, Oceanic conditions in the eastern equatorial Pacific during the onset of ENSO in the Holocene, Quat. Res. 60 (2003) 142–148.
[76] R. Bradley, R. Yuretich, B. Weingarten, Studies of modern climate, in: R. Yuretich (Ed.), Late Quaternary Climatic Fluctuations of the Venezuelan Andes, Dept. of Geosciences, Univ. of Massachusetts, Amherst, MA, 1991, pp. 45–62.
[77] J.F. Adkins, K. McIntyre, D.P. Schrag, The salinity, temperature, and $\delta^{18}O$ of the glacial deep ocean, Science 298 (2002) 1769–1773.
[78] W.R. Peltier, On eustatic sea level history: last Glacial Maximum to Holocene, Quat. Sci. Rev. 21 (2002) 377–396.
[79] M.B. Abbott, B.B. Wolfe, A.P. Wolfe, G.O. Seltzer, R. Aravena, B.G. Mark, P.J. Polissar, D.T. Rodbell, H.D. Rowe, M. Vuille, Holocene paleohydrology and glacial history of the central Andes using multiproxy lake sediment studies, Palaeogeogr. Palaeoclimatol. Palaeoecol. 194 (2003) 123–138.